

Preparation and photodynamic bactericidal effects of curcumin- β -cyclodextrin complex

Danning Lai^{a,1}, Arong Zhou^{a,1}, Bee K Tan^b, Yibin Tang^a, Siti Sarah Hamzah^c, Zhigang Zhang^d, Shaoling Lin^{a,e,*}, Jiamiao Hu^{a,e,*}

^a Engineering Research Centre of Fujian-Taiwan Special Marine Food Processing and Nutrition, Ministry of Education, Fuzhou 350002, China

^b Department of Cardiovascular Sciences and Diabetes Research Centre, University of Leicester, Leicester LE1 7RH, United Kingdom

^c Institute for Medical Research, Ministry of Health Malaysia, Jalan Pahang, 50588 Kuala Lumpur, Malaysia

^d State Key Laboratory of Food Safety Technology for Meat Products, Xiamen 361100, China

^e College of Food Science, Fujian Agriculture and Forestry University, Fuzhou 350002, China

ARTICLE INFO

Keywords:

Photodynamic sterilization

Curcumin

β -cyclodextrin

ABSTRACT

To overcome the poor water solubility of curcumin, a curcumin- β -cyclodextrin (Cur- β -CD) complex was prepared as a novel photosensitizer. Fourier-transform infrared spectroscopy (FT-IR), differential scanning calorimetry (DSC), and X-ray diffraction (XRD) were used to verify the formation of Cur- β -CD. Furthermore, the ROS generation capacity and photodynamic bactericidal effect were measured to confirm this Cur- β -CD complex kept photodynamic activity of curcumin. The result showed Cur- β -CD could effectively generate ROS upon blue-light irradiation. The plate count assay demonstrated Cur- β -CD complex possess desirable photodynamic antibacterial effect against food-borne pathogens including *Staphylococcus aureus*, *Listeria monocytogenes* and *Escherichia coli*. The cell morphology determined by scanning electron microscope (SEM) and transmission electron microscope (TEM) showed Cur- β -CD could cause cell deformation, surface collapse and cell structure damage of the bacteria, resulting in the leakage of cytoplasmic; while agarose gel electrophoresis and SDS-PAGE further illustrated the inactivation mechanisms by Cur- β -CD involve bacterial DNA damage and protein degradation.

1. Introduction

In recent decades, food safety and security has become a major global issue. Food-borne pathogens could endanger food safety and cause food-borne illnesses. Food safety issues caused by food-borne pathogens have become one of the most prominent health problems all over the world (Xu et al., 2014). Among food-borne pathogens, *Escherichia coli* (*E. coli*), *Listeria monocytogenes* (*L. monocytogenes*) and *Staphylococcus aureus* (*S. aureus*) are several common spoilage bacteria, and how to inhibit those in food has become a research focus around the world.

The sterilization methods currently used in the food industry include thermal sterilization, antibiotic sterilization, ultrahigh pressure, irradiation, pulsed light, and pulsed electric field, etc. (Li & Farid, 2016). Traditional thermal sterilization technology has difficulty in maintaining the original flavor and nutrition of food, while antibiotic sterilization methods can lead to drug resistance and thus rapidly phased out (Calero-

Caceres & Muniesa, 2016). Meanwhile, ultrahigh voltage, irradiation, pulsed light, and pulsed electric field still face a number of obstacles (such as high equipment costs, high energy consumption, and low processing capacity) before they can be widely applied.

As a novel non-thermal sterilization technology, photodynamic technology (PDT) has become an innovative sterilization method in the food industry because of its advantages of being highly efficient, cost effective, and environmental friendly (Zheng et al., 2020). Indeed, the inhibitory effect of PDT on *E. coli* and *S. aureus* has been increasingly studied. For example, the methylene blue activation of red lights at the wavelength of 635 nm could kill *E. coli* by more than 6-log and more than 99.99999% of *S. aureus* (Hasenleutner & Plaetzer, 2019); while Song et al. (Song et al., 2020) reported 5-aminolevulinic acid (ALA)-mediated PDT has significant bactericidal effect against methicillin-resistant staphylococcus aureus (MRSA).

Curcumin, a natural pigment, has been approved as a food additive

* Corresponding authors at: Engineering Research Centre of Fujian-Taiwan Special Marine Food Processing and Nutrition, Ministry of Education, Fuzhou 350002, China.

E-mail addresses: shaoling.lin@fafu.edu.cn (S. Lin), jiamiao.hu@fafu.edu.cn (J. Hu).

¹ Contributed equally to the article.

by World Health Organization and U.S. Food and Drug Administration (Anand et al., 2007; Zhang et al., 2013). Curcumin has been demonstrated as an effective photosensitizer to sterilize and inhibit bacteria by a number of studies. Corrêa et al. showed that curcumin-mediated PDT (Cur-PDT) was found to be able to reduce the contamination level of *S. aureus* on the surface of meat and fruit without obvious changes in food appearance and quality (Corrêa et al., 2020). Tao et al. also showed that Cur-PDT had good bactericidal efficacy against *E. coli* on the surface of fresh-cut apples, and the concentrations of curcumin and the illumination time were the main factors affecting bactericidal ability (Tao et al., 2019). Chai et al. found that Cur-PDT could effectively reduce the survival rate of *L. monocytogenes* on the surface of fresh-cut pears, thus maintaining the quality of pears (Chai et al., 2021). However, low water solubility of curcumin greatly limited its application in the use of PDT treatments in the food industry. Moreover, curcumin can rapidly decompose when the pH is higher than 7.12. To overcome these problems, studies have shown that a range of carrier molecules can be used to encapsulate curcumin, such as liposome (Kolter et al., 2019), nanoparticles (Huang et al., 2020), emulsion (Calahorra et al., 2020), and cyclodextrin (Marcolino et al., 2011; Mangolim et al., 2014), et al.

β -cyclodextrin (β -CD) is a cyclic oligosaccharide. Its exterior is relatively hydrophilic, while its interior is hydrophobic due to the shielding effect of C—H, making it to be a good candidate for encapsulating natural active compounds such as curcumin (Eid et al., 2010). A study showed that if the clathrate compound of curcumin and β -CD is formed, the solubility of curcumin can be increased by 104 times and the hydrolysis stability can be increased by more than 500 times (Tønnesen et al., 2002). At present, a number of β -CD derivatives such as methyl- β -CD, sulfobutylether- β -CD and hydroxypropyl- β -CD have been prepared and approved as pharmaceutical ingredients since substitution of the hydrogen bond-forming hydroxyl groups in β -CD results in a dramatic improvement in aqueous solubility. Notably, although parent β -CD has a relatively low aqueous solubility, which is widely used in the food industry due to its good safety record, wide availability and reasonable prices (Szente & Szejtli, 2004).

Therefore, to improve the water solubility and stability of curcumin, curcumin- β -CD complex (Cur- β -CD) was prepared and studied in this paper. Fourier-transform infrared spectroscopy (FT-IR), differential scanning calorimetry (DSC), and X-ray diffraction (XRD) were used to characterize the formation of the Cur- β -CD complex. Moreover, to confirm whether the Cur- β -CD complex still has antimicrobial photosensitive activity, its ROS generation ability and photodynamic inactivation of *S. aureus* (G^+), *L. monocytogenes* (G^+) and *E. coli* (G^-) were measured; the inactivation mechanisms of Cur- β -CD against food-borne bacteria were also explored.

2. Materials and methods

2.1. Material

Curcumin and β -CD were purchased from TCI Shanghai (China). Acetone, potassium bromide (KBr), phosphate buffered solution (PBS) and ethyl alcohol absolute were purchased from Sinopharm Chemical Reagent Co., Ltd (China). Dimethyl sulfoxide (DMSO) and glutaric dialdehyde were purchased from Shanghai Macklin Biochemical Co., Ltd (China). 2',7'-Dichlorodihydrofluorescein diacetate (DCF-DA) was purchased from Sigma-Aldrich. *S. aureus* (CICC 10201), *L. monocytogenes* (CICC 21633) and *E. coli* (CICC 10899) were obtained from China Center of Industrial Culture Collection. Plate count agar (PCA) and nutrient broth medium were purchased from Qingdao Haibo Biological Technology Co., Ltd (China). Bacterial Genomic DNA Extraction Kit was purchased from Omega Biotek Ltd. All other reagents were analytical grade.

2.2. Preparation of Cur- β -CD complex

Cur- β -CD composite photosensitizer was prepared based on the method described by Jahed et al. ADDIN EN.CITE (Jahed et al., 2014) with slight modifications. Four hundred milligrams of β -CD and 120 mg of curcumin powder were dissolved in deionized water (80 mL) and acetone (5 mL), respectively. The curcumin solution was added into the β -CD aqueous solution with continuous stirring. The mixture was stirred at room temperature in the dark for 24 h without capping to evaporate the acetone. Then, the solution was centrifuged (1000 rpm, 5 min) and the supernatant of the Cur- β -CD with high water solubility was recovered by freeze drying. Finally, the Cur- β -CD was refrigerated at 4 °C.

2.3. Fourier-transform infrared spectroscopy (FT-IR)

The infrared spectrum of samples was obtained by FT-IR. In brief, the samples were weighed and ground with KBr in a certain ratio (1:100, w/w) and then tested by compression method using Fourier-transform infrared spectrometer (TENSORII, Bruker, Germany). The scanning range was 400 ~ 4000 cm^{-1} , the scanning frequency was 32 times, and the resolution was 4 cm^{-1} (Sukhtezari et al., 2017).

2.4. X-ray diffraction analysis (XRD)

XRD pattern of Cur- β -CD was recorded at room temperature on an X-ray diffractometer (D8advance, Bruker, Germany). The acceleration voltage was set to 40 kV, the current intensity was 40 mA, the wavelength was 0.1546 nm, the scanning speed was 2°/min, and the scanning range was $2\theta = 3^\circ \sim 60^\circ$ (Huang et al., 2017; Wei et al., 2020).

2.5. Differential scanning calorimetry (DSC)

The DSC curves of samples were analyzed by synchronous thermal analyzer (STA449F, NETZSCH (Shanghai) Machinery and Instruments Co., Ltd (China)). Each sample (2 mg ~ 5 mg) was weighed in a closed aluminum pan before being heated from 30 °C to 220 °C at a rate of 10 °C/min with a nitrogen flow of 30 mL/min. An empty sealed pot was used as a reference.

2.6. Detection of reactive oxygen species (ROS)

As described in a previous report (Ganguly et al., 2020), 2',7'-Dichlorodihydrofluorescein diacetate (DCF-DA) was used as a detection probe to monitor the ROS production of the Cur- β -CD upon blue LED lights illumination. In brief, DCF-DA probe solution (50 μL) was added into 1 mL of Cur- β -CD (100 μM) solution. The mixture was illuminated at 425 nm and the fluorescence intensity of the solution was recorded every 10 s.

2.7. Determination of antibacterial effects

The photodynamic inactivation effects was determined as described in a previous study (Hu et al., 2018) with slight modifications. In brief, Cur- β -CD solution at different concentrations (0, 0.5%, 1%, 1.5%, 2%) were added into 1 mL of bacterial suspension (with a concentration of 10^7 CFU/mL) in 24-well plates. The plates were incubated in the dark for 15 min and then exposed to blue LED light for 0–75 min. Ten-fold series of dilutions were prepared, and 100 μL of each dilution gradient homogenate was aspirated on the PCA plate which was applied with a sterile applicator stick. The plates were incubated at 37 °C for 24 h to form viable colony units, while a blank control was prepared. Finally, plate colonies were counted and the inactivation rate was calculated according to formula (1). Where N_1 is the number of bacterial colonies in the experimental group upon PDT treatment, and N_0 is the number of bacterial colonies in the control group.

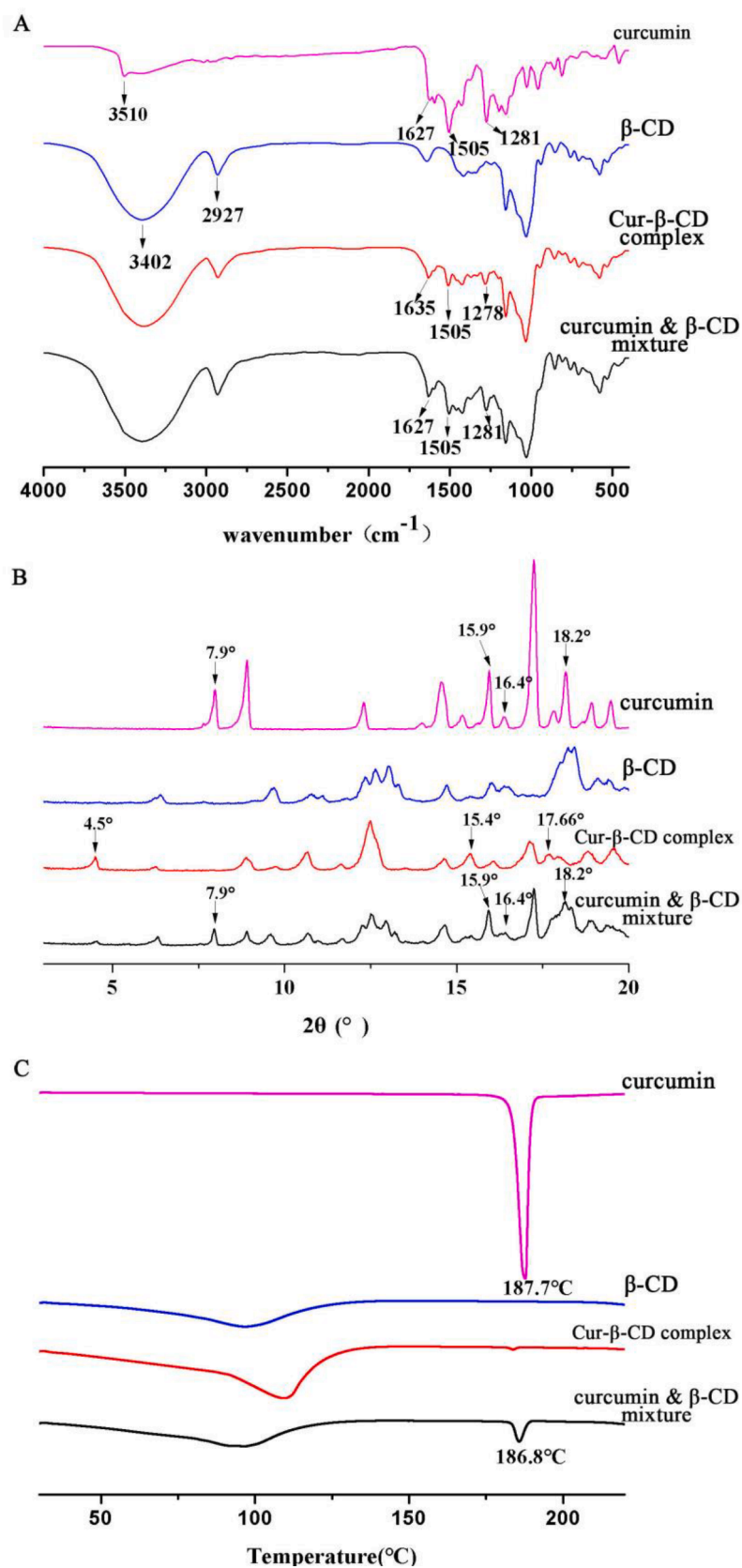


Fig. 1. FT-IR spectra (A), X-ray diffraction patterns (B), DSC Curves (C) of curcumin, β -CD, Cur- β -CD complex and curcumin & β -CD mixture.

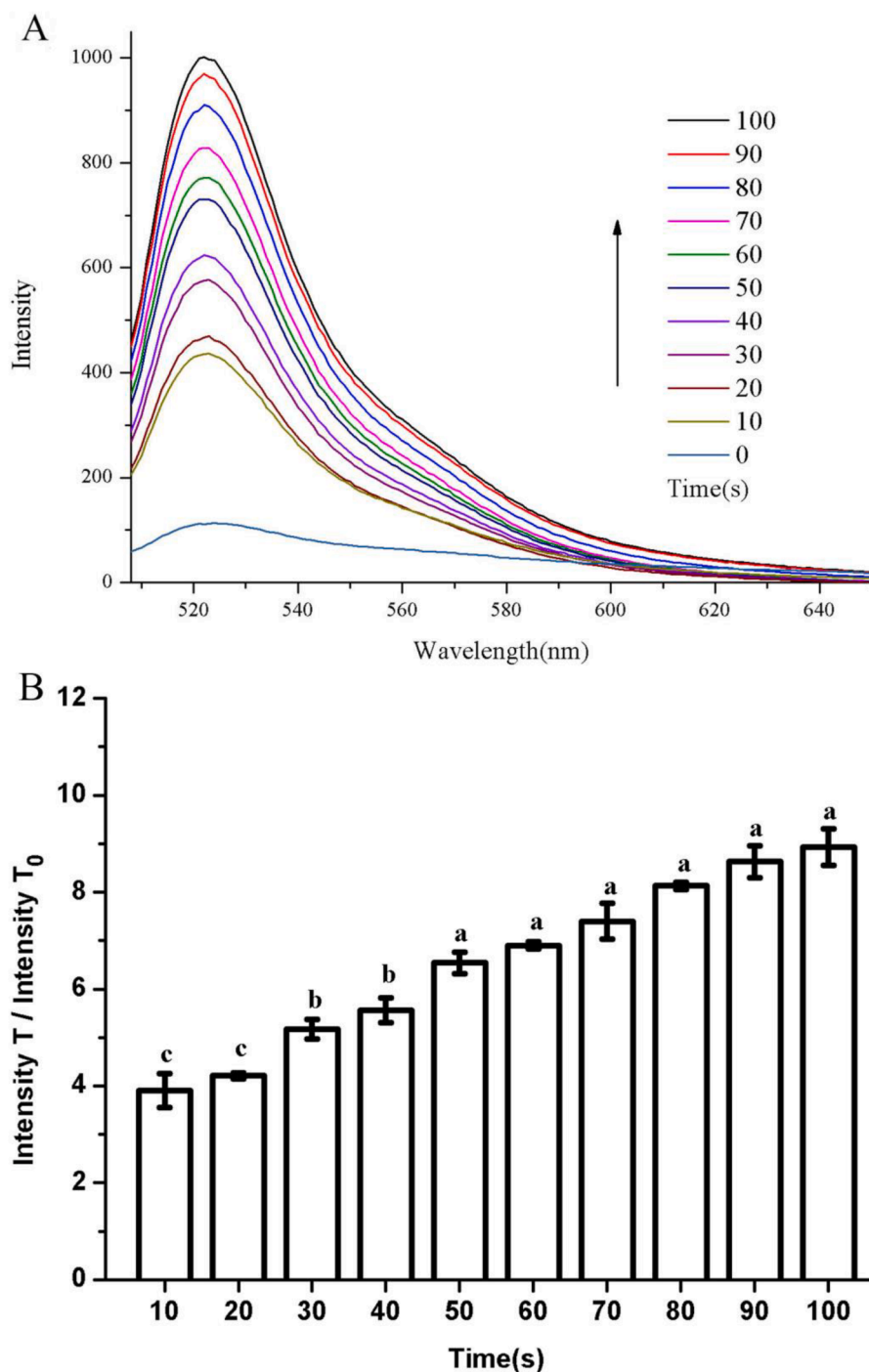


Fig. 2. (A) FL spectra of Cur-β-CD and DCF-DA mixture irradiation at different illumination time (0–100 s). (B) Enhancement of fluorescence intensity of DCF under different illumination time (at wavelength 523 nm). Intensity T is the Intensity value from 10 s to 100 s; Intensity T₀ is the initial Intensity value at 0 s. Different letters indicate statistically significant differences based on one-way ANOVA with Tukey's test ($P < 0.05$).

$$\text{Inactivation rate}(\%) = \frac{N_0 - N_t}{N_0} \times 100\%$$

(1)

samples were viewed using a SEM (SIGMA 500, Carl Zeiss, Germany) under 10000x magnification with a constant voltage of 15 kV.

2.8. Scanning electron microscope analysis (SEM)

The bacteria were immobilized with 2.5% glutaraldehyde and washed twice with PBS. Then the bacteria were successively dehydrated with 25%, 50%, 75% and 95% (v/v) aqueous ethanol, and finally with anhydrous ethanol. The bacterial samples were ion sputtered prior to SEM observation (Mishra and Padhy, 2017). After gold spraying, the

2.9. Transmission electron microscope analysis (TEM)

Bacteria were treated according to the TEM pretreatment method of Lin et al (Lin et al., 2018). TEM analysis was carried out in a JEM-F200 unit (JEOL Ltd., Tokyo, Japan), using 80 kV of accelerating voltage.

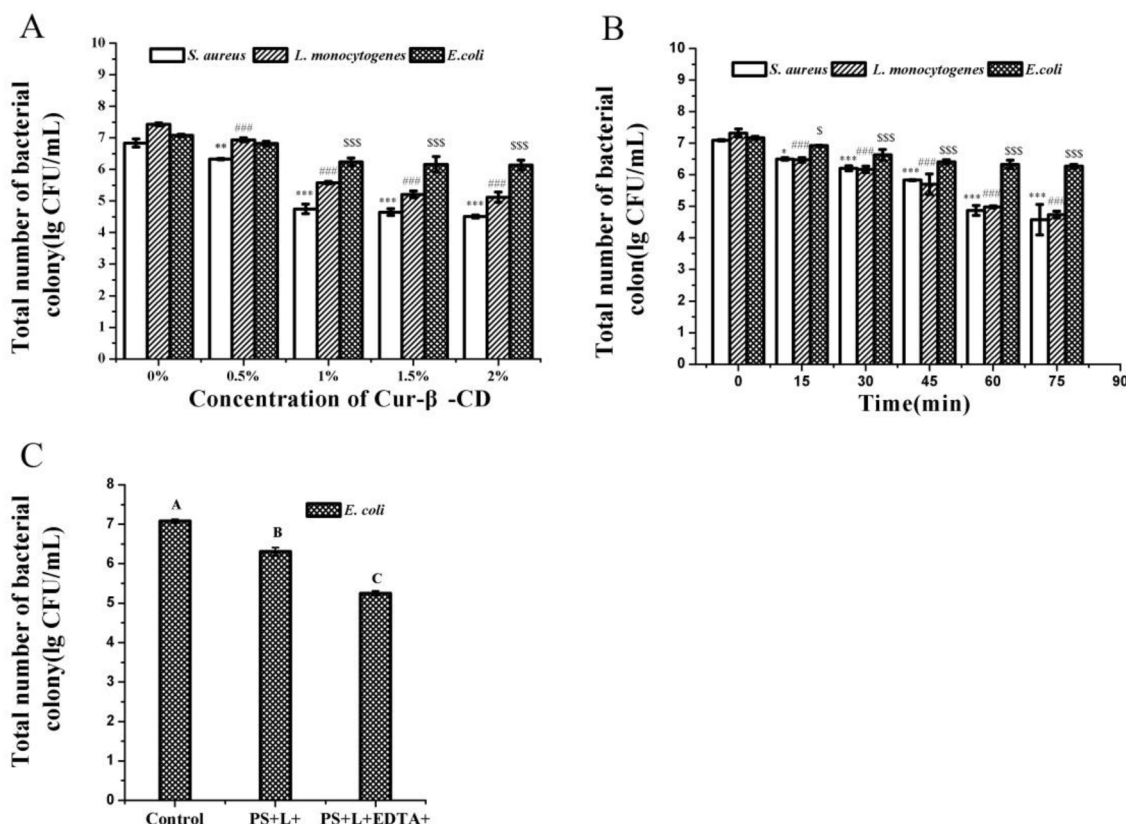


Fig. 3. (A & B) Effect of Cur-β-CD concentration and light irradiation time on antibacterial effects. *S. aureus*, *L. monocytogenes* and *E. coli* were treated with Cur-β-CD (0%-2%), and irradiated for 0–75 min (1%). *, $P < 0.05$, **, $P < 0.01$, ***, ###, \$\$\$, $P < 0.001$ based on one-way ANOVA with Dunnett's test compared to control (0%, 0 min) (*: *S. aureus*; #: *L. monocytogenes*; \$: *E. coli*). (C) Effect of Cur-PDT with EDTA on antibacterial effects. *E. coli* were treated with Cur-β-CD (1%) and irradiated for 60 min with or without EDTA. Different letters represent significant differences based on one-way ANOVA with Tukey's test ($P < 0.05$).

2.10. Determination of cytoplasmic leakage

The cytoplasmic leakage induced by Cur-β-CD mediated PDT were measured according to the method reported by Rout et al (Rout et al., 2017). In brief, the bacterial suspension after PDT treatment was filtered through a membrane with 0.22 μm pore size. The filtrate was collected and its absorbance at 260 nm and 280 nm were determined.

2.11. Agarose gel electrophoresis

Briefly, bacterial DNA was extracted with the DNA extraction kit (Omega Biotek, Norcross, GA, USA), according to the manufacturer's instructions, and analyzed by the horizontal agarose gel electrophoresis (The voltage of the electrophoresis apparatus was set to 100 V and the time was set as 30 min; the buffer used for electrophoresis was Tris-acetate-EDTA buffer.). The gel was stained with ethidium bromide and visualized using Bio-Rad ChemiDoc™ MP Imaging System (Bio-Rad, Hercules, CA, USA).

2.12. Sodium dodecyl sulphate–polyacrylamide gel electrophoresis (SDS-PAGE)

After Cur-β-CD mediated PDT treatment, bacterial pellets were collected in a 1.5 mL Eppendorf tubes by centrifugation at 10000g for 1 min at 4 °C. The supernatant was discarded and each pellet was re-suspended in 40 μL of 1 × SDS gel-loading buffer followed by heating in boiling water for 3 min. The samples were once again centrifuged at 10000g for 1 min at 4 °C again and the supernatant was analyzed on 12% SDS-PAGE. After electrophoresis, the gel was stained with Coomassie Brilliant Blue (Beyotime Biotechnology, Shanghai, China).

2.13. Data statistics and analysis

All assays were performed at least in triplicate, and the results were presented as mean ± SD. Graphpad Prism software was used to analyze the statistically significant differences using one-way analysis of variance (ANOVA) followed by Tukey's test and Dunnett's test ($P < 0.05$).

3. Results

3.1. Cur-β-CD complex characterization by FT-IR, XRD, and DSC

The infrared spectrum, X-ray diffraction patterns, DSC curves of curcumin, β-CD, Cur-β-CD complex and curcumin & β-CD mixture are shown in Fig. 1. As illustrated in Fig. 1A, in the curcumin spectrum, the characteristic absorption peak at 3510 cm⁻¹ was caused by the telescopic vibration of phenol O–H; and the peaks at 1627 cm⁻¹ and 1505 cm⁻¹ of curcumin correspond to the telescopic vibration of the benzene ring, the C=O and C=C vibrations, respectively (Kolev et al., 2005). The characteristic absorption peaks of FT-IR of β-CD at 3402 cm⁻¹, 2927 cm⁻¹, 1167 cm⁻¹ and 1032 cm⁻¹ correspond to the telescopic vibrations of O–H, C–H, C–O–C and C–O, respectively (Rao et al., 2021). The curcumin peak at 1281 cm⁻¹ was divided into three weak peaks between 1278 cm⁻¹ and 1361 cm⁻¹ in the infrared spectrum of Cur-β-CD, indicating that β-CD might interact with the benzene ring on the enol side of the curcumin molecule. In the Cur-β-CD spectrum, the peak at 1627 cm⁻¹ in the curcumin spectrum moved to 1635 cm⁻¹ in Cur-β-CD complex but not in the spectrum of mixture, indicating a change in the benzene ring of the compound. In addition, all the characteristic peaks (such as the O-methylated phenol group) of curcumin almost disappeared (1505–1281 cm⁻¹), and only a weak vibration was observed at

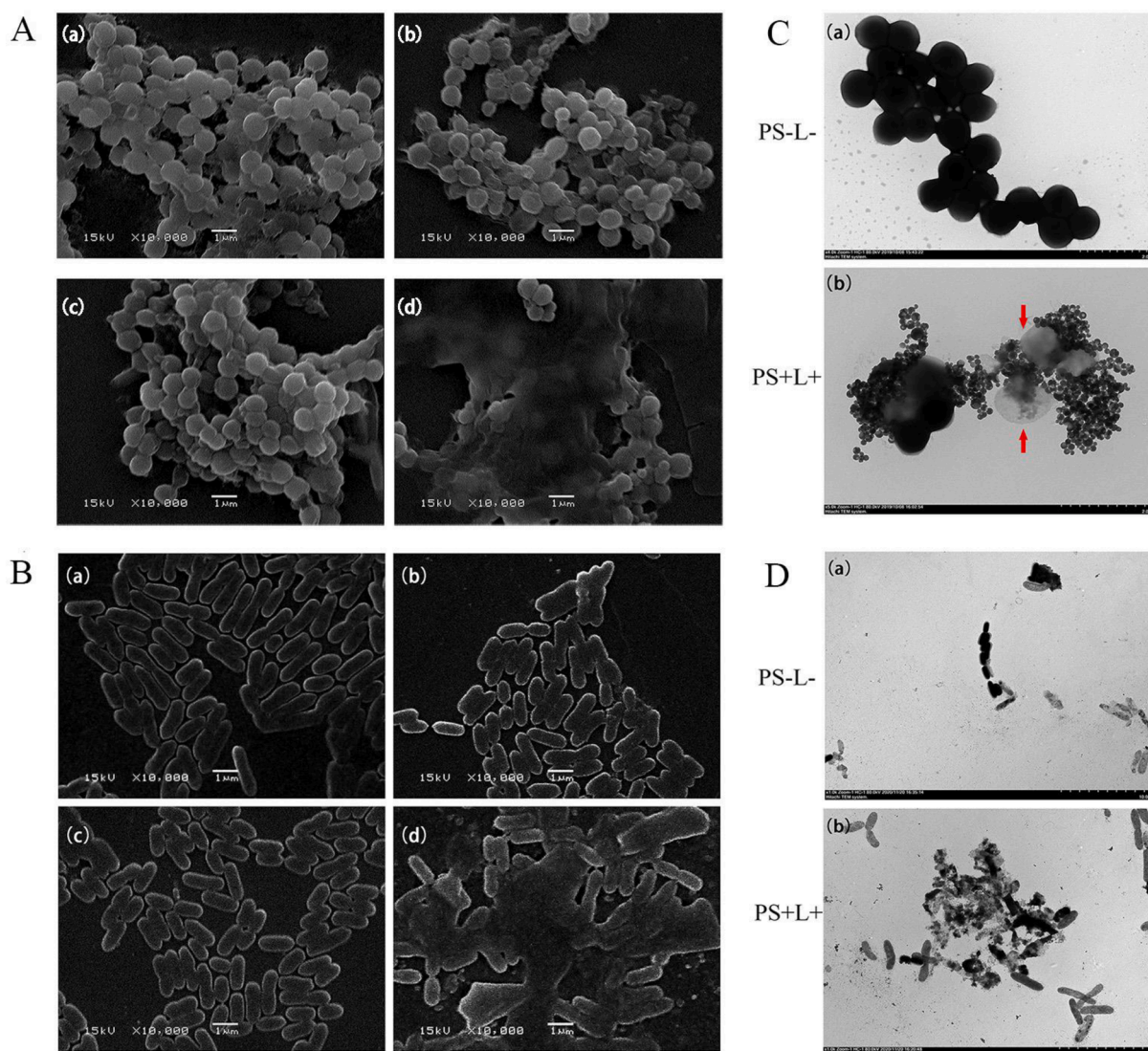


Fig. 4. (A & B) SEM images of *S. aureus* (A) and *L. monocytogenes* (B) in PS-L- group (a), PS-L + group (b), PS + L- group (c) and PS + L + group (d). Magnifications: $\times 10000$; (C & D) TEM images of *S. aureus* (C) and *L. monocytogenes* (D) in PS-L- group (a) and PS + L + group (b). Arrows indicated the cytoplasmic leakage of some cells in *S. aureus*.

1505 cm^{-1} in the Cur- β -CD spectrum, indicating that curcumin combined with β -CD and the compound still maintained the structure of C=O and C=C. Furthermore, the infrared spectrum of Cur- β -CD and β -CD were similar and no significant spectral difference was observed. The above changes also illustrated the formation of Cur- β -CD complex. Similarly, XRD analysis also demonstrated the diffraction pattern of curcumin & β -CD mixture was the approximate superposition of curcumin and β -CD diffraction peaks; while Cur- β -CD complex displayed the appearance of new diffraction peaks (at $2\theta = 4.5^\circ$, 15.4° and 17.66°) with some characteristic diffraction peaks of curcumin disappearing (at $2\theta = 7.9^\circ$, 15.9° , 16.4° and 18.2°) (Fig. 1B), indicating the existence of new solid crystalline phases corresponding to inclusions with the same properties (Mangolim et al., 2014). In addition, in the DSC curve of Cur- β -CD (Fig. 1C), the endothermic peak of the phase transition corresponding to the melting point of curcumin disappeared completely, and the endothermic peak belonging to β -CD increased from 96.8°C to 109.4°C . These phenomena may be due to curcumin molecules entering the cavity of β -CD by replacing water molecules (Yallapu et al., 2010), which also indicated the formation of Cur- β -CD complexes.

3.2. ROS production capacity of Cur- β -CD complex upon light activation

The photosensitizer could aid the generation of reactive oxygen species (ROS) through photochemical reactions. Therefore, fluorogenic dye DCF-DA was used to detect the capacity of ROS production of Cur- β -CD. As shown in Fig. 2A, with the prolongation of the illumination time (0 s \sim 100 s), the fluorescence intensity of DCF at 523 nm increased gradually, indicating that Cur- β -CD could produce ROS upon irradiation. Quantification of fluorescence showed that the fluorescence intensity of DCF increases 7.9 ± 0.38 times within 100 s (Fig. 2B). Taken together, these experimental results demonstrated that Cur- β -CD could generate ROS rapidly and effectively upon the irradiation of blue LED lights, which is essential for Cur- β -CD complex exerting its photodynamic antibacterial activity.

3.3. Photodynamic bactericidal effects of Cur- β -CD complex

Next, the photodynamic bactericidal effects of Cur- β -CD complex against Gram-positive bacteria and Gram-negative bacteria were evaluated. The representative Gram-positive bacteria *S. aureus* and *L. monocytogenes* and Gram-negative bacteria *E. coli* were selected for

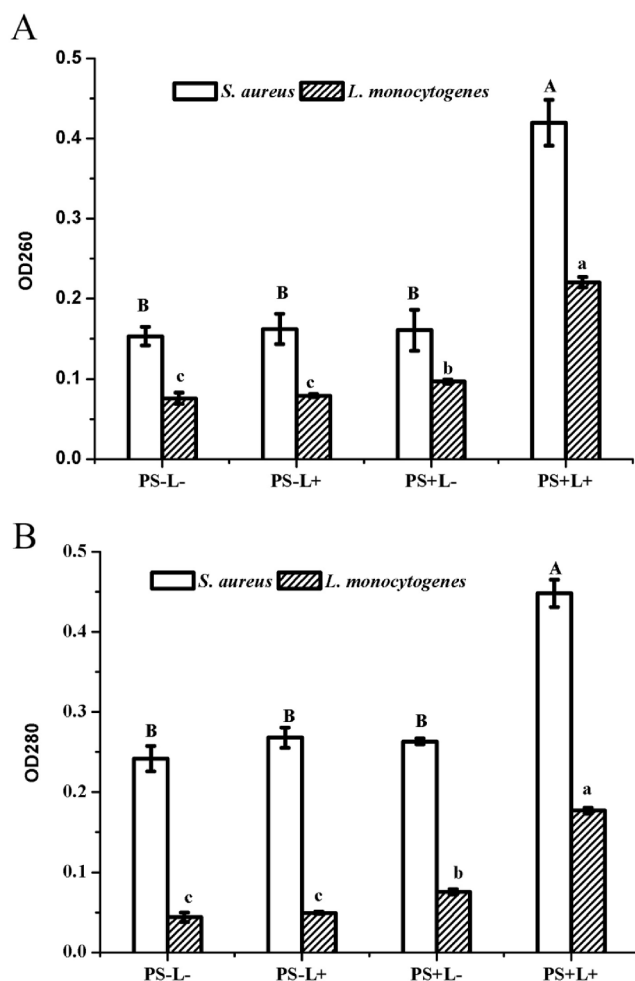


Fig. 5. Release of 260 nm (A) and 280 nm (B) cytoplasmic contents in the filtrate of the suspension of *S. aureus* and *L. monocytogenes*. Different letters represent significant differences based on one-way ANOVA with Tukey's test ($P < 0.05$).

photodynamic sterilization experiments. The effects of Cur- β -CD concentration and illumination time on the antibacterial activity against *S. aureus*, *L. monocytogenes* and *E. coli* are shown in Fig. 3. In general, increasing Cur- β -CD concentrations or length of illumination resulted in more effective bactericidal effects. Illumination with 1% concentration of Cur- β -CD for 60 min led to $99.77 \pm 0.18\%$ and $98.66 \pm 0.26\%$ reduction in *S. aureus* and *L. monocytogenes* viability, respectively, and $85.78 \pm 4.89\%$ decrease in *E. coli* viability (reduce by about 0.84 lg CFU/mL) were observed after Cur- β -CD mediated PDT treatment. When Cur- β -CD concentration was increased to 2% or the time was extended to 75 min, the antibacterial effect further increased slightly. In contrast, curcumin at any tested concentration did not show obvious killing effects on *S. aureus*, *L. monocytogenes* and *E. coli* when there was no light. Furthermore, our results also showed the bactericidal effects of Cur- β -CD on *S. aureus* and *L. monocytogenes* (G^+) were significantly higher than that on *E. coli* (G^-). To improve the antibacterial effect of Cur- β -CD on *E. coli*, EDTA were added; the results revealed that the bactericidal effect of Cur- β -CD against *E. coli* was markedly augmented by the addition of EDTA (Fig. 3C).

3.4. Inactivation mechanisms of Cur- β -CD complex against *S. Aureus* and *L. Monocytogenes*

Given our findings that Cur- β -CD showed significant antibacterial effects on *S. aureus* and *L. monocytogenes*, we further explored the

inactivation mechanisms of Cur- β -CD mediated PDT on on these bacteria (G^+).

3.4.1. Morphological changes

Morphological changes of *S. aureus* and *L. monocytogenes* were determined by SEM and TEM, after being treated with 1% Cur- β -CD in combination with light. As shown in Fig. 4A, cells of the blank control group (PS-L- group) had smooth surface morphologies and intact cell membranes, which exhibited a good staphylococcal structure ($<1 \mu\text{m}$ in diameter). Meanwhile, the cells in PS-L + group (without photosensitizer) and PS + L- group (without illumination) still had smooth cell surfaces. In contrast, cell deformation and surface collapse occurred on bacterial cells in the photodynamic group (PS + L +). Similarly, the characteristic rod-shaped structure of *L. monocytogenes* could be viewed in the bacteria of control groups (PS-L-; PS-L+; and PS + L-); while cells appeared distorted after incubation with Cur- β -CD and exposure to light (Fig. 4B). TEM also demonstrated similar findings that the bacteria in the PS-L- group maintained the normal morphological characteristics, while most of the *S. aureus* and *L. monocytogenes* cells lysed resulting in leakage of cytoplasmic contents upon Cur- β -CD mediated photodynamic treatment in the PS + L + group (Fig. 4C and Fig. 4D).

3.4.2. Cytoplasmic material leakage

Since the damage to the integrity of the cell membrane is an important mechanism by which photodynamic action inactivates microorganisms (Liu et al., 2017), the release of intracellular components was next measured as an indicator of damaged bacterial membrane (Yi et al., 2010). Here, bacterial membrane permeability was assessed by measuring the leakage of intracellular biomolecules (protein and nucleic acid), which have maximum absorption peaks at 260 nm and 280 nm, respectively. As shown in Fig. 5, compared with the blank control group (PS-L-), OD₂₆₀ and OD₂₈₀ of bacterial filtrates in the PS-L + and PS + L- groups did not show significant differences, while in the PS + L + groups these absorbance values significantly increased, indicating Cur- β -CD upon light activation could damage the cell structure of *S. aureus* and *L. monocytogenes*, resulting in enhanced cytoplasmic leakage.

3.4.3. Genomic DNA damage

To further reveal the lethal effect of Cur- β -CD based photodynamic sterilization against *S. aureus* and *L. monocytogenes*, the damage of bacterial DNA was studied by agarose gel electrophoresis. As can be seen from Fig. 6A and Fig. 6B, genomic DNA of *S. aureus* and *L. monocytogenes* extracted from the control groups (PS-L-; PS-L + and PS + L-) did not show significant DNA cleavage (lanes 1, 2 and 3), indicating that DNA damage was not induced by light alone or by 1% Cur- β -CD. However, isolated genomic DNA from *S. aureus* and *L. monocytogenes* upon photodynamic treatment became a smear on the gel (lane 4), with less of the DNA band remaining. This experimental result suggested that Cur- β -CD-mediated photosensitization resulted in the destruction of genomic DNA, which may be another possible reason the bactericidal effects on *S. aureus* and *L. monocytogenes*.

3.4.4. Protein degradation

To further reveal protein damage, SDS-PAGE was used to study protein obtained from *S. aureus* and *L. monocytogenes* treated with Cur- β -CD mediated photodynamic sterilization. As shown in Fig. 6C and Fig. 6D, the protein bands of the bacteria in the blank control groups (PS-L-; PS-L + and PS + L-) were clear and sharp, but the protein bands in the PS + L + groups were vague and had a smear pattern. Compared with the PS-L- group, most of the protein bands became dim or even disappeared, with only several shallow bands (eg. ~ 180 kDa, 75 kDa, 25–35 kDa, and 17 kDa in Fig. 6C and ~ 60 –70 kDa, 50 kDa, 20 kDa in Fig. 6D) that were not completely degraded in the PS + L + groups. Generally, the widespread disappearance of proteins suggested that the proteins were degraded on a large scale, indicating Cur- β -CD combined with light could degrade most of the proteins in *S. aureus* and

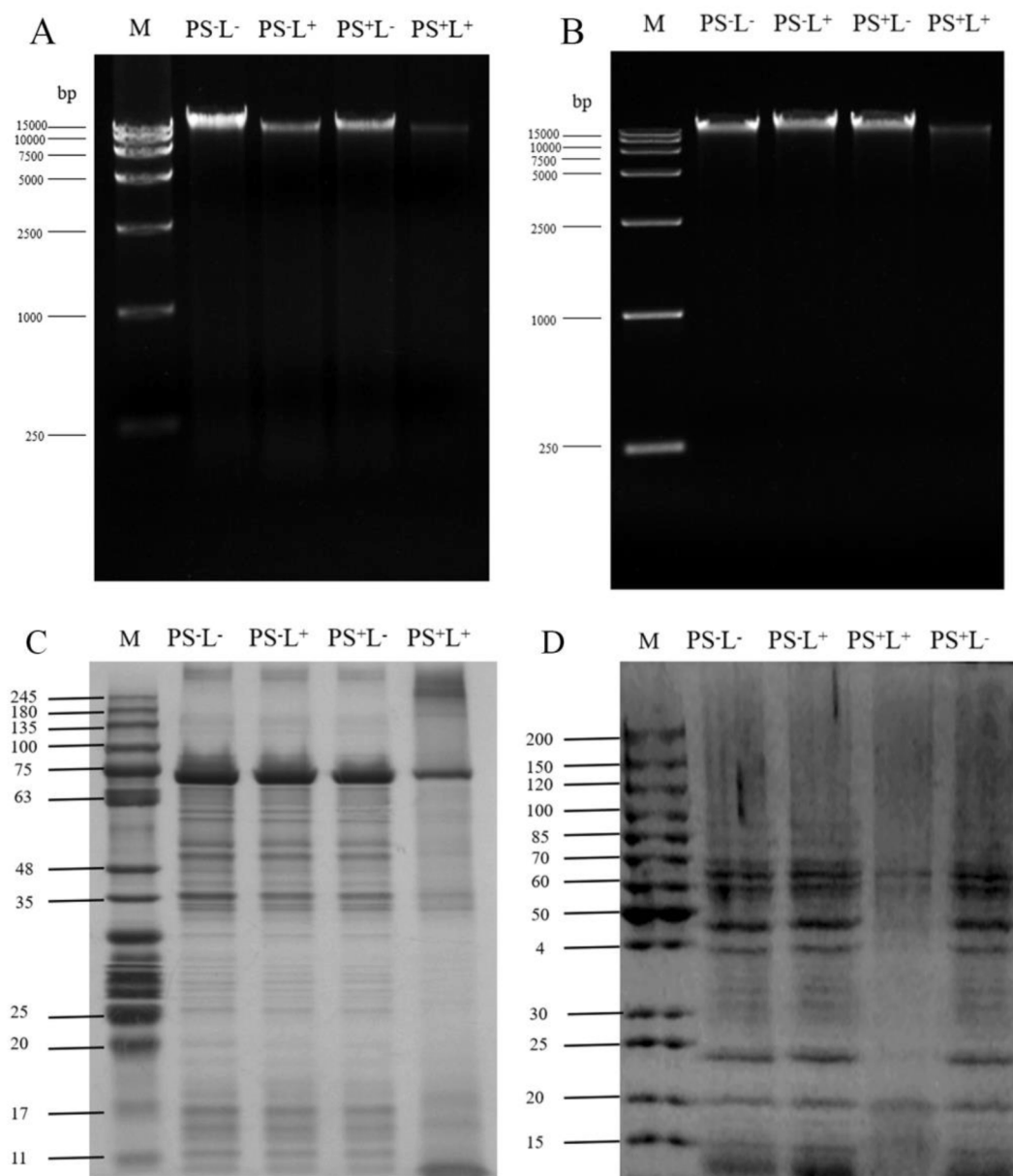


Fig. 6. (A & B) Agarose gel electrophoresis analysis of *S. aureus* (A) and *L. monocytogenes* (B) DNA damage. Lane M: DNA Marker (DL15000); Lane PS-L⁻: bacteria treated with water in the dark; Lane PS-L⁺: bacteria treated with water and irradiated for 60 min; Lane PS⁺L⁻: bacteria treated with Cur- β -CD (1%) in the dark; Lane PS⁺L⁺: bacteria treated with Cur- β -CD (1%) with light for 60 min. (C&D) SDS-PAGE analysis of protein degradation of *S. aureus* (C) and *L. monocytogenes* (D) upon photodynamic treatment. Lane M: Protein Marker; Lane PS-L⁻: bacteria treated with water in the dark; Lane PS-L⁺: bacteria treated with water and irradiated for 60 min; Lane PS⁺L⁻: bacteria treated with Cur- β -CD (1%) in the dark; Lane PS⁺L⁺: bacteria treated with Cur- β -CD (1%) with light for 60 min.

L. monocytogenes during the photoactivation.

4. Discussion

In the current study, curcumin- β -cyclodextrin complex photosensitizer (Cur- β -CD) was prepared, and its antibacterial effects against several typical food-borne pathogenic bacteria were studied. Curcumin is a natural photosensitizer with a good safety profile, approved as a food supplement by FDA (Anand et al., 2007; Zhang et al., 2013). However, its potential as a potential food preservative has been greatly limited by its low water solubility. Indeed, a number of studies have been conducted to improve this shortcoming. For example, Santana et al. synthesized the curcumin and superparamagnetic iron oxide nanoparticles (SPIONPs) conjugate as a novel photosensitizer and confirmed its bactericidal activity against *S. aureus* upon blue LED light

illumination. (Santana et al., 2020). In addition, curcumin-encapsulated liposomes are also a promising strategy to design curcumin derivatives as novel photosensitizers with enhanced solubility, increased bioavailability, and good storage stability. However, the antibacterial effects of curcumin-loaded liposomes are affected by its concentration as curcumin may separate from the bilayer and degrade at low concentrations (Kolter et al., 2019). Notably, a previous study showed that β -cyclodextrin could greatly enhance the curcumin solubility (Marcolino et al., 2011), which has great potential as a promising food additive due to its simple synthesis process and low manufacturing costs. Indeed, several studies have been performed showing that Cur- β -CD complexes can be added into vanilla ice cream (Mangolim et al., 2014) or yogurt (Marcolino et al., 2011) to achieve better color with good sensorial acceptability. However, there are few studies to explore the photodynamic and bactericidal properties of Cur- β -CD and its application in the

field of food safety.

In our study, we show that the formation of Cur- β -CD complex was verified by FT-IR and X-ray diffraction. The results of infrared spectroscopy demonstrated that the interactions occurred between β -CD and the benzene ring on the enol side of the curcumin molecule, and nearly all of the characteristic peaks of curcumin disappeared, which confirms the formation of Cur- β -CD. Our XRD data also showed that the disappearance of the characteristic diffraction peaks of curcumin and new diffraction peaks being observed in Cur- β -CD. In addition, the results of DSC indicated that curcumin successfully entered the cavity of β -CD to form Cur- β -CD complexes.

We also confirmed that curcumin still had photosensitizer properties after being compounded with β -CD through ROS generation, using fluorescein DCF-DA to detect ROS generation under light stimulation. Furthermore, we demonstrated that several typical foodborne bacteria can be effectively sterilized by Cur- β -CD mediated PDT treatment. The antibacterial effect of Cur- β -CD was also enhanced by increasing the concentrations of Cur- β -CD or the prolongation of light time. Our results further showed higher bactericidal effects of Cur- β -CD against *S. aureus* and *L. monocytogenes* (G^+) compared to *E. coli* (G^-). This is consistent with previous studies that Gram-negative bacteria are more resistant to photodynamic treatment because their outer membranes have a complex structure of two lipid molecules, including a peptidoglycan layer and a dense membrane outside the cell wall. In contrast, the outer membrane of Gram-positive bacteria is more porous, wherein photosensitizer molecules and toxic ROS generated by photosensitizers could easily penetrate (Maisch et al., 2004; Nagata et al., 2012). A marked increase observed in the bactericidal effects of Cur- β -CD against *E. coli* by the addition of EDTA was also in line with previous findings, plausibly by disorganizing the outer membranes of Gram-negative bacteria (Bertolini et al., 1990).

Furthermore, the antibacterial mechanism analysis suggested that Cur- β -CD mediated PDT may result in the disruption of cell membranes resulting in leakage of cytoplasmic contents. Indeed, this observation is consistent with reports from Agel et al. (Agel et al., 2019), in which it was also found that *S. aureus* treated with curcumin-loaded nanoparticles in combination with LED radiation resulted in severe morphological defects and changes in the overall appearance of bacterial cells. Additionally, ROS generated from Cur- β -CD mediated PDT could also degrade bacterial genomic DNA and proteins of *S. aureus* and *L. monocytogenes*, suggesting that the photodynamic bactericidal mechanisms of Cur- β -CD found in our study is consistent with that reported in previous studies (Kanmani & Rhim, 2014; Hu et al., 2018) showing that curcumin combined with blue LED activation could lead to bacterial DNA damage and protein degradation.

5. Conclusion

We present novel data showing that Cur- β -CD complexes have photosensitizer properties with bactericidal effects on *S. aureus* and *L. monocytogenes*. Moreover, we found that similar to Cur-PDT, the mechanisms of Cur- β -CD based photodynamic inactivation against *S. aureus* and *L. monocytogenes* involve the morphological destruction, the leakage of cytoplasmic contents, the degradation of the proteins as well as genomic DNA breakages.

Future research to progress the translation application of Cur- β -CD into the food industry should focus on optimizing experimental conditions and parameters, testing the inhibition effect on other food-borne pathogenic bacteria, and further enhancing the bactericidal effects against Gram-negative bacteria as well as to study the impact of Cur- β -CD mediated PDT on food quality and sensorial acceptability.

CRedit authorship contribution statement

Danning Lai: Data curation, Formal analysis, Validation, Writing - original draft. **Arong Zhou:** Methodology, Investigation. **Bee K Tan:**

Writing - review & editing. **Yibin Tang:** . **Siti Sarah Hamzah:** Conceptualization, Funding acquisition. **Zhigang Zhang:** . **Shaoling Lin:** Conceptualization, Funding acquisition, Supervision. **Jiamiao Hu:** Funding acquisition, Supervision, Writing - review & editing.

Declaration of Competing Interest

The authors declare that they have no known competing financial interests or personal relationships that could have appeared to influence the work reported in this paper.

Acknowledgments

The authors are grateful to the National Natural Science Foundation of China (31801649); Natural Science Foundation of Fujian Province (2020I0010, 2020I0012); "13th Five Year Plan" National Key Research and Development Project (2016YFD0400403); the Research Fund for Taiwan-Straits Postdoctoral Exchange Program (2018B003); Science and Technology Major Project of Zhangzhou (ZZ2019ZD18); Special Funds for Science and Technology Innovation of FAFU (CXZX2019100S; CXZX2019101S) for financial support.

Appendix A. Supplementary data

Supplementary data to this article can be found online at <https://doi.org/10.1016/j.foodchem.2021.130117>.

References

- Agel, M. R., Baghdan, E., Pinnapireddy, S. R., Lehmann, J., Schäfer, J., & Bakowsky, U. (2019). Curcumin loaded nanoparticles as efficient photoactive formulations against gram-positive and gram-negative bacteria. *Colloids and Surfaces B: Biointerfaces*, 17, 460–468. <https://doi.org/10.1016/j.colsurfb.2019.03.027>.
- Anand, P., Kunnumakkara, A. B., Newman, R. A., & Aggarwal, B. B. (2007). Bioavailability of curcumin: Problems and promises. *Molecular Pharmaceutics*, 4(6), 807–818. <https://doi.org/10.1021/mp700113r>.
- Bertolini, G., Rossi, F., Valduga, G., Jori, G., & Lier, J. v. (1990). Photosensitizing activity of water- and lipid-soluble phthalocyanines on *Escherichia coli*. *FEMS Microbiology Letters*, 71(1–2), 149–155. [10.1016/0378-1097\(90\)90048-U](https://doi.org/10.1016/0378-1097(90)90048-U).
- Calahorra, A. A., Wang, Y. Q., Boesch, C., Zhao, Y. S., & Sarkar, A. (2020). Pickering emulsions stabilized by colloidal gel particles complexed or conjugated with biopolymers to enhance bioaccessibility and cellular uptake of curcumin. *Current Research in Food Science*, 3, 178–188. <https://doi.org/10.1016/j.crf.2020.05.001>.
- Calero-Caceres, W., & Muniesa, M. (2016). Persistence of naturally occurring antibiotic resistance genes in the bacteria and bacteriophage fractions of wastewater. *Water Research*, 95, 11–18. <https://doi.org/10.1016/j.watres.2016.03.006>.
- Chai, Z., Zhang, F., Liu, B., Chen, X., & Meng, X. (2021). Antibacterial mechanism and preservation effect of curcumin-based photodynamic extends the shelf life of fresh-cut pears. *LWT*, 142, 110941. <https://doi.org/10.1016/j.lwt.2021.110941>.
- Corrêa, T. Q., Blanco, K. C., Garcia, É. B., Perez, S. M. L., Chianfrone, D. J., Moraes, V. S., & Bagnato, V. S. (2020). Effects of ultraviolet light and curcumin-mediated photodynamic inactivation on microbiological food safety: A study in meat and fruit. *Photodiagnosis and Photodynamic Therapy*, 30, 1–7. <https://doi.org/10.1016/j.pdpdt.2020.e04036>.
- Eid, E. E. M., Abdul, A. B., Suliman, F. E. O., Sukari, M. A., Rasedee, A., & Fatah, S. S. (2010). Characterization of the inclusion complex of zerumbone with hydroxypropyl- β -cyclodextrin. *Carbohydrate Polymers*, 83(4), 1707–1714. <https://doi.org/10.1016/j.carbpol.2010.10.033>.
- Ganguly, D., Santra, R. C., Mazumdar, S., Saha, A., Karmakar, P., & Das, S. (2020). Radioprotection of thymine and calf thymus DNA by an azo compound: Mechanism of action followed by DPPH radical quenching & ROS depletion in WI 38 lung fibroblast cells. *Heliyon*, 6(5), Article e04036. <https://doi.org/10.1016/j.heliyon.2020.e04036>.
- Hasenleutner, M., & Plaetzer, K. (2019). In the right light: Photodynamic inactivation of microorganisms using a LED-based illumination device tailored for the antimicrobial application. *Antibiotics*, 9(1), 1–13. <https://doi.org/10.3390/antibiotics9010013>.
- Hu, J., Lin, S., Tan, B. K., Hamzah, S. S., Lin, Y., Kong, Z., ... Zeng, S. (2018). Photodynamic inactivation of *Burkholderia cepacia* by curcumin in combination with EDTA. *Food Research International*, 111, 265–271. <https://doi.org/10.1016/j.foodres.2018.05.042>.
- Huang, W. N., Wang, L. H., Wei, Y. Q., Cao, M. N., Xie, H. J., & Wu, D. (2020). Fabrication of lysozyme/k-carrageenan complex nanoparticles as a novel carrier to enhance the stability and in vitro release of curcumin. *International Journal of Biological Macromolecules*, 146, 444–452. [10.1016/j.ijbiomac.2020.01.004](https://doi.org/10.1016/j.ijbiomac.2020.01.004).
- Huang, X., Dai, Y., Cai, J., Zhong, N., Xiao, H., McClements, D. J., & Hu, K. (2017). Resveratrol encapsulation in core-shell biopolymer nanoparticles: Impact on

- antioxidant and anticancer activities. *Food Hydrocolloids*, 64, 157–165. <https://doi.org/10.1016/j.foodhyd.2016.10.029>.
- Jahed, V., Zarzabi, A., Bordbar, A.-khalegh., & Hafezi, M. S. (2014). NMR (^1H , ROESY) spectroscopic and molecular modelling investigations of supramolecular complex of β -cyclodextrin and curcumin. *Food Chemistry*, 165, 241–246. <https://doi.org/10.1016/j.foodchem.2014.05.094>.
- Kanmani, P., & Rhim, J.-W. (2014). Physicochemical properties of gelatin/silver nanoparticle antimicrobial composite films. *Food Chemistry*, 148, 162–169. <https://doi.org/10.1016/j.foodchem.2013.10.047>.
- Kolev, T. M., Velcheva, E. A., Stamboliyska, B. A., & Spitteller, M. (2005). DFT and experimental studies of the structure and vibrational spectra of curcumin. *International Journal of Quantum Chemistry*, 102(6), 1069–1079. [https://doi.org/10.1002/\(ISSN\)1097-461X10.1002/qua.v102:610.1002/qua.20469](https://doi.org/10.1002/(ISSN)1097-461X10.1002/qua.v102:610.1002/qua.20469).
- Kolter, M., Wittmann, M., Köll-Weber, M., & Süß, R. (2019). The suitability of liposomes for the delivery of hydrophobic drugs – A case study with curcumin. *European Journal of Pharmaceutics and Biopharmaceutics*, 140, 20–28. <https://doi.org/10.1016/j.ejpb.2019.04.013>.
- Li, X., & Farid, M. (2016). A review on recent development in non-conventional food sterilization technologies. *Journal of Food Engineering*, 182, 33–45. <https://doi.org/10.1016/j.jfoodeng.2016.02.026>.
- Lin, L., Gu, Y. L., Li, C. Z., Vittayapadung, S., & Cui, H. Y. (2018). Antibacterial mechanism of ϵ -Poly-lysine against *Listeria monocytogenes* and its application on cheese. *Food Control*, 91, 76–84. <https://doi.org/10.1016/j.foodcont.2018.03.025>.
- Liu, B., Xue, Y., Zhang, J., Han, B., Zhang, J., Suo, X., ... Shi, H. (2017). Visible-light-driven $\text{TiO}_2/\text{Ag}_3\text{PO}_4$ heterostructures with enhanced antifungal activity against agricultural pathogenic fungi *Fusarium graminearum* and mechanism insight. *Environmental Science: Nano*, 4(1), 255–264. <https://doi.org/10.1039/C6EN00415F>.
- Maisch, T., Szeimies, R.-M., Jori, G., & Abelsa, C. (2004). Antibacterial photodynamic therapy in dermatology. *Photochemical & Photobiological Sciences*, 3(10), 907–917. <https://doi.org/10.1039/b407622b>.
- Mangolim, C. S., Moriaki, C., Nogueira, A. C., Sato, F., Baesso, M. L., Neto, A. M., & Matioli, G. (2014). Curcumin- β -cyclodextrin inclusion complex: Stability, solubility, characterisation by FT-IR, FT-Raman, X-ray diffraction and photoacoustic spectroscopy, and food application. *Food Chemistry*, 153, 361–370. <https://doi.org/10.1016/j.foodchem.2013.12.067>.
- Marcolino, V. A., Zanin, G. M., Durrant, L. R., Benassi, M. D. T., & Matioli, G. (2011). Interaction of curcumin and bixin with β -cyclodextrin: Complexation methods, stability, and applications in food. *Journal of Agricultural and Food Chemistry*, 59(7), 3348–3357. <https://doi.org/10.1021/jf104223k>.
- Mishra, M. P., & Padhy, R. N. (2017). Antibacterial activity of green silver nanoparticles synthesized from *Anogeissus acuminata* against multidrug resistant urinary tract infecting bacteria in vitro and host-toxicity testing. *Journal of Applied Biomedicine*. <https://doi.org/10.1016/j.jab.2017.11.003>.
- Nagata, J. Y., Hioka, N., Kimura, E., Batistela, V. R., Terada, R. S. S., Graciano, A. X., ... Hayacibara, M. F. (2012). Antibacterial photodynamic therapy for dental caries: Evaluation of the photosensitizers used and light source properties. *Photodiagnosis and Photodynamic Therapy*, 9(2), 122–131. <https://doi.org/10.1016/j.pdpdt.2011.11.006>.
- Rao, S.-qi., Sun, M.-ling., Hu, Y., Zheng, X.-feng., Yang, Z.-quan., & Jiao, X.-an. (2021). ϵ -Polylysine-coated liposomes loaded with a β -CD inclusion complex loaded with carvacrol: Preparation, characterization, and antibacterial activities. *LWT*, 146, 111422. <https://doi.org/10.1016/j.lwt.2021.111422>.
- Rout, B., Liu, C. H., & Wu, W. C. (2017). Photosensitizer in lipid nanoparticle: a nano-scaled approach to antibacterial function. *Scientific Reports*, 7(1), 7892–7892. 10.1038/s41598-017-07444-w.
- de Santana, W. M. O. S., Caetano, B. L., de Annunzio, S. R., Pulcinelli, S. H., Ménager, C., Fontana, C. R., & Santilli, C. V. (2020). Conjugation of superparamagnetic iron oxide nanoparticles and curcumin photosensitizer to assist in photodynamic therapy. *Colloids and Surfaces B: Biointerfaces*, 196, 111297. <https://doi.org/10.1016/j.colsurfb.2020.111297>.
- Song, J. H., QianYu, H., Sun, M. J., Liao, H. B., & Li, L. N. (2020). Inhibitory effect of 5-aminolevulinic acid photodynamic therapy on methicillin-resistant *Staphylococcus aureus*. *Chinese Journal of Nosocomiology*, 30(02), 161–164. 10.11816/cn.ni.2020-183285.
- Sukhtezari, S., Almasi, H., Pirsas, S., Zandi, M., & Pirouzifard, M. (2017). Development of bacterial cellulose based slow-release active films by incorporation of *Scrophularia striata* Boiss. extract. *Carbohydrate Polymers*, 156, 340–350. <https://doi.org/10.1016/j.carbpol.2016.09.058>.
- Szente, L., & Szejtli, J. (2004). Cyclodextrins as food ingredients. *Trends in Food Science & Technology*, 15(3–4), 137–142. <https://doi.org/10.1016/j.tifs.2003.09.019>.
- Tao, R., Zhang, F., Tang, Q.-juan., Xu, C.-shan., Ni, Z.-J., & Meng, X.-hong. (2019). Effects of curcumin-based photodynamic treatment on the storage quality of fresh-cut apples. *Food Chemistry*, 274, 415–421. <https://doi.org/10.1016/j.foodchem.2018.08.042>.
- Tønnesen, H. H., Måsson, M., & Loftsson, T. (2002). Studies of curcumin and curcuminoids. XXVII. Cyclodextrin complexation: Solubility, chemical and photochemical stability. *International Journal of Pharmaceutics*, 244(1), 127–135. [https://doi.org/10.1016/S0378-5173\(02\)00323-X](https://doi.org/10.1016/S0378-5173(02)00323-X).
- Wei, Y., Wang, C., Liu, X., Mackie, A., Zhang, L., Liu, J., ... Gao, Y. (2020). Impact of microfluidization and thermal treatment on the structure, stability and in vitro digestion of curcumin loaded zein-propylene glycol alginate complex nanoparticles. *Food Research International*, 138, 109817. <https://doi.org/10.1016/j.foodres.2020.109817>.
- Xu, F. X., Liu, S. Y., Lan, T. F., Wang, Y. H., & Feng, X. Q. (2014). Pollution situation and coping strategies of foodborne pathogens. *Food Research And Development*, 35(01), 98–101. <https://doi.org/10.3969/j.issn.1005-6521.2014.01.027>.
- Yallapu, M. M., Jaggi, M., & Chauhan, S. C. (2010). β -Cyclodextrin-curcumin self-assembly enhances curcumin delivery in prostate cancer cells. *Colloids and Surfaces B: Biointerfaces*, 79(1), 113–125. <https://doi.org/10.1016/j.colsurfb.2010.03.039>.
- Yi, S. M., Zhu, J. L., Fu, L. L., & Li, J. R. (2010). Tea polyphenols inhibit *Pseudomonas aeruginosa* through damage to the cell membrane. *International Journal of Food Microbiology*, 144(1), 111–117. 10.1016/j.ijfoodmicro.2010.09.005.
- Zhang, C.-Y., Zhang, L., Yu, H.-X., Bao, J.-D., Sun, Z., & Lu, R.-R. (2013). Curcumin inhibits invasion and metastasis in K1 papillary thyroid cancer cells. *Food Chemistry*, 139(1–4), 1021–1028. <https://doi.org/10.1016/j.foodchem.2013.02.016>.
- Zheng, B. D., Lin, S. L., Zeng, S. X., Hu, J. M., & Lai, D. N. (2020). Photodynamic technology and its application in food industry. *Journal of Food Science and Biotechnology*, 05, 6–15. <https://doi.org/10.3969/j.issn.1673-1689.2020.05.002>.